bioRxiv preprint doi: https://doi.org/10.1101/443978; this version posted October 15, 2018. The copyright holder for this preprint (which was not certified by peer review) is the author/funder, who has granted bioRxiv a license to display the preprint in perpetuity. It is made available under aCC-BY 4.0 International license.

The effect of butyrate-supplemented parenteral nutrition on intestinal defence mechanisms and the parenteral nutrition-induced shift in the gut microbiota

Short title: Butyrate-supplemented parenteral nutrition and intestinal defence mechanisms

Jirsova Z[1], Heczkova M[1], Dankova H[1], Malinska H[1], Videnska P[2], Vespalcova H[2], Micenkova L[2], Bartonova L[3], Sticova E[3], Lodererova A[3], Prefertusová L.[3], Sekerkova A[4], Cahova M[1,*]

[1]Department of Experimental Medicine, Institute for Clinical and Experimental Medicine, Prague, CR
[2]RECETOX, Faculty of Science, Masaryk University, Brno, CR
[3]Clinical and Transplant Pathology Department, Institute for Clinical and Experimental Medicine, Prague, CR
[4]Prevedig, Prague, CR

* Corresponding author

E-mail: monika.cahova@ikem.cz

bioRxiv preprint doi: https://doi.org/10.1101/443978; this version posted October 15, 2018. The copyright holder for this preprint (which was not certified by peer review) is the author/funder, who has granted bioRxiv a license to display the preprint in perpetuity. It is made available under aCC-BY 4.0 International license.

Abstract

Butyrate produced by the intestinal microbiota is essential for proper functioning of the intestinal immune system. Total dependence on parenteral nutrition (PN) is associated with numerous adverse effects, including severe microbial dysbiosis and loss of important butyrate producers. We hypothesised that a lack of butyrate produced by the gut microbiota may be compensated by its supplementation in PN mixtures. We tested whether *i.v.* butyrate administration would (a) positively modulate intestinal defence mechanisms and (b) counteract PN-induced dysbiosis. Male Wistar rats were randomised to chow, PN, and PN supplemented with 9 mM butyrate (PN+But) for 12 days. Antimicrobial peptides, mucins, tight junction proteins and cytokine expression were assessed by RT-qPCR. T-cell subpopulations in mesenteric lymph nodes (MLN) were analysed by flow cytometry. Microbiota composition was assessed in caecum content. Butyrate supplementation resulted in increased expression of tight junction proteins (*ZO-1, claudin-7, E-cadherin*), antimicrobial peptides (*Defa 8, Rd5, RegIIIγ*) and lysozyme in the ileal mucosa. Butyrate partially alleviated PN-induced intestinal barrier impairment and normalised IL-4, IL-10 and IgA mRNA expression. PN administration was associated with an increase in Tregs in MLN, which was normalised by butyrate. Butyrate increased the total number of CD4+ and decreased a relative amount of CD8+ memory T cells in MLN. Lack of enteral nutrition and PN administration led to a shift in caecal microbiota composition. Butyrate did not reverse the altered expression of most taxa but did influence the abundance of some potentially beneficial/ pathogenic genera, which might contribute to its overall beneficial effect.

bioRxiv preprint doi: https://doi.org/10.1101/443978; this version posted October 15, 2018. The copyright holder for this preprint (which was not certified by peer review) is the author/funder, who has granted bioRxiv a license to display the preprint in perpetuity. It is made available under aCC-BY 4.0 International license.

Introduction

Parenteral nutrition (PN) represents a life-saving treatment in patients with intestinal failure. However, PN and/or lack of enteral feeding are often associated with serious adverse effects, including impaired mucosal homeostasis, loss of immune reactivity (1), compromised intestinal barrier function and generalised sepsis (2).

Proper gut barrier function depends on the integrity of physical barriers, i.e. tight junction proteins and adequate mucin production, sufficient production of antimicrobial compounds by Paneth cells and maintaining an optimal balance between immune tolerance to commensal microbiota and the defence against invading pathogens (3). Lack of enteral feeding significantly affects all of these factors. Paneth cells, which are a specialised type of epithelial cell, release a spectrum of antimicrobial compounds when exposed to alloantigens (4). The absence of enteral feeding decreases mRNA and protein expression of typical Paneth cell antimicrobials like lysozyme, cryptidin-4 and secretory phospholipase A2, thus compromising their function (5, 6). The data concerning the effect of PN on the function of Paneth cells are inconclusive, as their antimicrobial functions have been shown to both increase (3) and decrease (7).

Goblet cells (GCs) continuously secrete glycoproteins (mucins) in order to repair and replace the intestinal mucus barrier (8). Until recently, GCs were considered relatively passive players in promoting intestinal homeostasis and the host defence. However, recent reports indicate that GCs are able to sense and respond to danger signals (such as bacterial pathogens) as well as modulate the composition of the gut microbiome by modifying mucin secretion (9). In a piglet model of enteral nutrition deprivation, GC expansion was established within a few days after the start of total or partial PN (10), which might reflect a higher degradation rate of the mucus layer, a lower rate of mucus secretion, or an altered rate of mucin turnover (11).

bioRxiv preprint doi: https://doi.org/10.1101/443978; this version posted October 15, 2018. The copyright holder for this preprint (which was not certified by peer review) is the author/funder, who has granted bioRxiv a license to display the preprint in perpetuity. It is made available under aCC-BY 4.0 International license.

These data indicate that starvation alters mucus dynamics in the small intestine, which may in turn affect the intestinal defence capacity (11, 12).

The gut microbiota has an irreplaceable role in the maturation of mucosal and systemic immunity (13-15). Depending on its composition, it may either promote a tolerogenic state in the intestinal mucosa (16-20) and instigate mechanisms preventing bacterial overgrowth or induce pro-inflammatory status associated with impaired gut barrier function (21). PN itself, together with a lack of enteral feeding, generates a significant shift in microbiota composition. In rodent models, PN and starvation are associated with decreased gut microbiota diversity, the enrichment of potentially pathogenic and inflammation-promoting species, and the depletion of beneficial anaerobes (3, 7, 22). Heneghan (7) hypothesises that the PN-associated shift in the gut microbiota may be part of a causal relationship with attenuated antimicrobial compound production.

As well as interacting directly with the host intestinal and immune cells, the gut microbiota may affect host intestinal homeostasis via fermentation products. Short-chain fatty acids (SCFA) have multiple beneficial effects on performance and intestinal health (23). SCFA are produced by the fermentation of soluble fibre. To target intestinal SCFA production, an often-used treatment is to supplement the diet with prebiotics (dietary fibre), probiotics (mostly *Lactobacillaceae* or *Bifidobacteriaceae*) or a combination of both. Unfortunately, this approach is not applicable to all situations. Particularly PN-dependent patients with short bowel syndrome often exhibit an increased abundance of *Lactobacillaceae* as well as a lack of butyrate producers in the gut. Therefore, prebiotic/probiotic supplementation may result in D-lactate acidosis or *Lactobacillus* sepsis. The alternative to prebiotic/probiotic treatment is the direct administration of butyrate either *per os* or intravenously. To our knowledge, no study has been published on the effect of i.v. butyrate on the microbiota in a PN context. The purpose of this study was to determine whether the

bioRxiv preprint doi: https://doi.org/10.1101/443978; this version posted October 15, 2018. The copyright holder for this preprint (which was not certified by peer review) is the author/funder, who has granted bioRxiv a license to display the preprint in perpetuity. It is made available under aCC-BY 4.0 International license.

supplementation of a nutrition mixture with butyrate (9 mM) in the absence of enteral feeding would affect immune function and gut microbiota composition. In order to examine this hypothesis, we used a rat model of total parenteral nutrition and assessed the effect of *i.v.* butyrate on Paneth cell function, mucin production, intestine-associated immune cells and the gut microbiome.

Materials and Methods

Animals and experimental design

Male Wistar rats (Charles River, initial weight 300-325 g) were kept in a temperature-controlled environment under a 12h light/dark cycle. For PN administration, the right jugular vein was cannulated with a Dow Corning Silastic drainage catheter (0.037 inch) as previously described (3). Control animals underwent the same operation. The catheter was flushed daily with TauroLock HEP-100 (TauroPharm GmbH, Waldbüttelbrunn, Germany). After the operation, the rats were housed individually and connected to a perfusion apparatus (Instech, PA, USA), which allows free movement. For the next 48 hours, the rats were given free access to a standard chow diet (SD, SEMED) and provided Plasmalyte (BAXTER Czech, Prague, CZ) via the catheter at increasing rates (initial rate: 1 ml/hr; goal rate: 4 ml/hr) in order to adapt to the increasing fluid load. Two days after the operation, the rats were randomly divided into three groups. Rats in the experimental groups (PN; PN+But) were provided PN (205 kcal. kg^{-1}. d^{-1}; 10 hrs per day; rate 4 ml. hr^{-1}; light period), the composition of which is given in Table S1. In the PN+But group, the PN mixture was supplemented with 9 mM butyrate. PN alone, PN+But or Plasmalyte was administered for 12 days. All experiments were performed in accordance with the Animal Protection Law of the Czech Republic 311/1997 in compliance with the Principles of Laboratory Animal Care (NIH Guide for the

bioRxiv preprint doi: https://doi.org/10.1101/443978; this version posted October 15, 2018. The copyright holder for this preprint (which was not certified by peer review) is the author/funder, who has granted bioRxiv a license to display the preprint in perpetuity. It is made available under aCC-BY 4.0 International license.

Care and Use of Laboratory Animals, 8th edition, 2013) and approved by the Ethical Committee of the Ministry of Health, CR (approval no. 53/2014).

Histological evaluation

Tissue samples (distal ileum, proximal colon) were fixed in 4% paraformaldehyde, embedded in paraffin blocks and routinely processed. Sections cut at 4-6 μm were stained with haematoxylin/eosin and examined with an Olympus BX41 light microscope.

Immunohistochemistry

Paraffin sections (4 μm) were deparaffinised in xylene and rehydrated in graded ethanol. Endogenous peroxidase was blocked, with proteinase K digestion (Dako, Glostrup, Denmark) used for antigen retrieval. The primary anti-lysozyme antibody (rabbit polyclonal, Dako, Glostrup, Denmark) was detected using Histofine Simple Stain Rat MAX PO (Nichirei, Japan). Lysozyme staining intensity was assessed by two independent blinded observers (scale 0 to 3), with average scores presented for each group.

Flow cytometry

Single cell suspensions from mesenteric lymph nodes (MLN) were obtained by gently fragmenting and filtering the tissues through 100 μm cell strainers (Sigma Aldrich), with lymphocytes isolated by centrifugation on Ficoll (ρ = 1.077 g/ml, GE Healthcare). Isolated cells were frozen and stored at -80°C until analysis. Prior to staining, the lymphocytes were thawed and incubated for two hours in RPMI 1640 + 10% FCS, 2mM L-glutamine, 1% Pen/Strep. Panels for both effector and regulatory T cells were stained simultaneously. First, cells were surface-stained using the following anti-rat antibodies: anti-CD45-FITC (OX-1,

bioRxiv preprint doi: https://doi.org/10.1101/443978; this version posted October 15, 2018. The copyright holder for this preprint (which was not certified by peer review) is the author/funder, who has granted bioRxiv a license to display the preprint in perpetuity. It is made available under aCC-BY 4.0 International license.

Thermo Fisher Scientific), anti-CD4-BV-786 (OX-35, BD Biosciences), anti-CD8α-PerCP-e710 (OX-8, Thermo Fisher Scientific), anti-CD62L-PE (OX-85, SONY) and anti-CD45RC-Alexa Fluor 647 (OX-22, SONY) for the effector T-cell panel, and anti-CD45-FITC, anti-CD4-BV-786 and anti-CD25-PE (OX-39, Thermo Fisher Scientific) for the regulatory T-cell panel. Second, the cells in both panels were fixed and permeabilised using an intracellular staining kit (Anti-Mouse/Rat Foxp3 Staining Set APC, Thermo Fisher Scientific) either with Foxp3 antibody (FJK-16s, regulatory T cells) or PBS (effector T cells) in conjunction with 15-min blocking using 2% normal rat serum (regulatory T cells only, Thermo Fisher Scientific). Immediately after staining with anti-Foxp3 mAb, the lymphocytes were analysed using the BD LSR II flow cytometer (BD Biosciences).

RT-qPCR

Pieces of the distal ileum (5-8 cm from the ileocaecal valve) were rapidly dissected, flushed first with cold saline and then with RNA later, opened along the mesenteric border and the mucosa was then scraped using a glass slide and immediately frozen in liquid nitrogen. To determine cytokine expression, Peyer's patches were dissected from the rest of the ileum. Total RNA was extracted using the RNeasy PowerMicrobiome Kit (Qiagen, Hilden, Germany). A DNAase step was included to avoid possible DNA contamination. A standard amount of total RNA (1600 ng) was used to synthesise first-strand cDNA with the High Capacity RNA-to-cDNA Kit (Applied Biosystems, Foster City, CA, USA). The RT-PCR amplification mixture (25ul) contained 1 ul template cDNA, SYBR Green Master Mix buffer (QuantiTect, Qiagen, Hilden, Germany) and 400nM (10 pmol/reaction) of sense and antisense primers. Primers were designed based on known rat sequences taken from the GeneBank Graphics database: *https://www.ncbi.nlm.nih.gov*. Primer design was performed with Primer3 software: http://www.frodo.wi.mit.edu (Table 1). The reaction was run on the

bioRxiv preprint doi: https://doi.org/10.1101/443978; this version posted October 15, 2018. The copyright holder for this preprint (which was not certified by peer review) is the author/funder, who has granted bioRxiv a license to display the preprint in perpetuity. It is made available under aCC-BY 4.0 International license.

ViiA 7 Real-Time PCR System (Thermo Fisher Scientific, USA). Results were analysed using SDS software, ver. 2.3 (Applied Biosystems, Foster City, CA, USA). The expression of genes of interest was normalised to the housekeeper gene Rplp2 and calculated using the ΔΔCt method.

Table 1. Primer sequences (5' - 3').

		sense (forward)	antisense (reverse)
Defa 8	NM_001033077.1	GGTCCAGGCTGATCACATTC	TTATGTCCTCCCTGGTGTCC
lysozyme	NM_012771.3	AAGGCATTCGAGCATGGGTG	TGAGAAAGAGACAGTGTGAGCTG
RegIII	NM_173097.1	GAGCCTCAGGATTTCTGAG	TCAAATGAGAGGAAGGAAGG
Muc3	XM_017598596.1	CAACGAAGAACAAGAAAACG	TGGGCTCTTCTGAATCTGG
Muc2	NM_173097.1	CCAATATCACCTGCCCTGAC	AGCAAGAACACCCATGATCC
Fcgbp	NM_001164657.2	TCTCCCCATGTCCCAACTG	GTTTGAATTCAGGGGCTCAG
IFNγ	NM_138880.2	CCAAGTTCGAGGTGAACAAC	CCAGAATTCTTCTTATTGGCACAC
IL-10	NM_012854.2	CTGCAGGACTTTAAGGGTTACTTG	TTCTCACAGGGGAGAAATCG
TNFα	NM_012675.3	ACGTCGTAGCAAACCACCAAG	TGTGGGTGAGGAGCACATAG
ZO-1	NM_001106266.1	TGTTCCTGTGAGTCCTTCAG	AAGGTGGGAGGATGCTATTG
Cldn7	NM_031702.1	CATCGTGGCAGGTCTTGCTG	GTGCACGGTATGCAGCTTTG
Igha	NC_005105.4	ATCCCACCATCTACCCACTGA	ATTGTTCCAGCGCTCGGCA
IL-4	NM_201270.1	CCACGGAGAACGAGCTCATC	GAGAACCCCAGACTTGTTCTTCA
Cdh1	NM_031334.1	GAAGACCAGGACTTTGATTTG	TCAGAACCACTCCCCTCATAG
Rplp2	NM_001030021.1	TCGCTCAGGGTGTTGGCAAG	AGGCCAAATCCCATGTCGTC

Determination of microbiota composition

Microbiota composition was determined in caecum content. All samples were frozen at -20 °C until required. DNA was isolated using the QIAamp PowerFecal DNA Kit (Qiagen). Extracted DNA was used as a template in amplicon PCR to target the hypervariable V4 region of the bacterial 16S rRNA gene. A 16S metagenomics library was prepared according to the Illumina 16S Metagenomic Sequencing Library Preparation protocol, with some

bioRxiv preprint doi: https://doi.org/10.1101/443978; this version posted October 15, 2018. The copyright holder for this preprint (which was not certified by peer review) is the author/funder, who has granted bioRxiv a license to display the preprint in perpetuity. It is made available under aCC-BY 4.0 International license.

modifications described below. Each PCR was performed in triplicate, with the primer pair consisting of Illumina overhang nucleotide sequences, an inner tag and gene-specific sequences (forward: TCGTCGGCAGCGTCAGATGTGTATAAGAGACAG-InnerTag-GTGYCAGCMGCCGCGGTAA; reverse: GTCTCGTGGGCTCGGAGATGTGTATAAGAGACAGC-InnerTag-GGACTACNVGGGTWTCTAAT) (24, 25). The Illumina overhang served to ligate the Illumina index and adapter. Each inner tag – a unique sequence of 7–9 bp – was designed to differentiate samples into groups. After PCR amplification, triplicates were pooled and the amplified PCR products determined by gel electrophoresis. PCR clean-up was performed with Agencourt AMPure XP beads (Beckman Coulter Genomics). Samples with different inner tags were equimolarly pooled based on fluorometrically measured concentrations using the Qubit® dsDNA HS Assay Kit (Invitrogen™, USA) and microplate reader (Synergy Mx, BioTek, USA). Pools were used as a template for the second PCR with Nextera XT indexes (Illumina, USA). Differently indexed samples were quantified using the KAPA Library Quantification Complete Kit (Kapa Biosystems, USA) and equimolarly pooled according to the measured concentration. The prepared library was checked with the 2100 Bioanalyzer Instrument (Agilent Technologies, USA), with concentrations measured by qPCR shortly prior to sequencing. The library was diluted to a final concentration of 8 pM with the addition of 20 % PhiX DNA (Illumina, USA). Sequencing was performed using the Miseq Reagent Kit v2 according to the manufacturer's instructions (Illumina, USA).

Data processing and statistical analysis

Sequencing data, i.e. raw sequences, were processed using standard bioinformatic procedures within QIIME 1.9.1 package (26). In short, these include quality filtering, chimera removal, open reference clustering and taxonomic identification based on the SILVA 123

bioRxiv preprint doi: https://doi.org/10.1101/443978; this version posted October 15, 2018. The copyright holder for this preprint (which was not certified by peer review) is the author/funder, who has granted bioRxiv a license to display the preprint in perpetuity. It is made available under aCC-BY 4.0 International license.

database and UCLUST algorithm (27). Raw sequences were filtered according to default quality requirements in QIIME 1.9.1 (-r: 3; -p: 0.75; -n:0; -q:3). Chimeras were detected and filtered using the UCHIME algorithm with the Gold database. Data were afterwards clustered at the 97% similarity threshold against SILVA database version 123. Representative sequences were aligned, and a phylogenetic tree was constructed and taxonomic identity determined by the USEARCH algorithm. The data were treated as compositional (proportions of total read count in each sample, non-rarefied) and prior to all statistical analyses were transformed using centered log-ratio transformation (28). Sequencing data are available from ENA database under the accession number PRJEB28521. All analyses were performed in R, version 3.4.2. (29).

Gene expression data and flow cytometry data are presented as mean ± SD. Statistical analysis was performed using the Kruskal-Wallis test with multiple comparisons. Differences were considered statistically significant at the level of $p<0.05$. For testing group pairwise differences in microbial composition, we applied ANOVA test with Tukey's honest significance. The statistical analyses were performed on each of the six taxonomy levels (Phylum, Class, Order, Family, Genus and OTUs) separately. The resulting p-values were adjusted for multiple hypothesis testing using the Benjamini-Hochberg procedure. Results were considered significant at FDR<=10%.Hierarchical clustering with Euclidean distance and the average-linkage algorithm was used to cluster microbial profiles in the heatmap and the radar chart.

Results

Ileal and colonic architecture

Compared with controls, we observed significantly reduced mucosal thickness in the ileum (550±40 vs 746±28 μm, $p<0.05$) and colon (886±90 vs 2750±110 μm, $p<0.01$) (Fig 1)

bioRxiv preprint doi: https://doi.org/10.1101/443978; this version posted October 15, 2018. The copyright holder for this preprint (which was not certified by peer review) is the author/funder, who has granted bioRxiv a license to display the preprint in perpetuity. It is made available under aCC-BY 4.0 International license.

252 in rats totally dependent on PN. Butyrate supplementation had no effect on these parameters
253 (ileum: 535±32; colon: 1020±103 µm).

254 **Fig 1. Histology of the intestinal mucosa**. Mucosal thickness was assessed in the small
255 intestine (ileum) and the large intestine (colon). Sections of intestinal tissues were stained
256 with H&E (magnification x100).

257

258 Butyrate stimulates Paneth cell function

259 To examine the potential Paneth cell alterations associated with butyrate administration,
260 we determined the expression of Paneth cell-produced compounds. First, we examined the
261 expression of lysozyme. Immunohistochemical staining confirmed its presence in Paneth cell
262 granules in the ileum in all groups (Fig 2). Based on staining intensity, PN administration
263 substantially increased lysozyme expression compared with controls (Fig 2B).
264 Supplementation of the PN mixture with butyrate resulted in the further elevation of
265 lysozyme-specific staining intensity (Fig 2C). Corresponding results were obtained at the
266 mRNA level (Fig 2E). Next, we determined the expression of other antimicrobial peptides,
267 i.e. α-defensins (Rd5, Defa8) and RegIIIγ (Figs 2F-H). Whereas PN alone had no effect, we
268 found significantly increased expression of all three compounds in the PN+But group. In
269 conclusion, our data show that supplementation of a PN mixture with butyrate is associated
270 with increased Paneth cell function, as measured by the expression of antimicrobial peptides.

271 **Fig 2. Host defence peptide proteins and mRNA expression in the ileum**. A-C: Lysozyme
272 staining, magnification x 200; D: lysozyme staining quantification; E: lysozyme mRNA
273 expression; F: RD5 mRNA expression; G: Defa8 mRNA expression; H: RegIIIγ mRNA
274 expression. mRNA expression is given as a fold change over the control group. Results are
275 presented using Tukey box-and-whisker plots as quartiles (25%, median, and 75%). $^{**}p < 0.01$
276 PN vs control; $^{\dagger\dagger}p < 0.01$; $^{\dagger\dagger\dagger}p < 0.001$ PN+But vs control; $^{\#}p < 0.05$, $^{\#\#\#}p < 0.001$ PN+But vs PN.

bioRxiv preprint doi: https://doi.org/10.1101/443978; this version posted October 15, 2018. The copyright holder for this preprint (which was not certified by peer review) is the author/funder, who has granted bioRxiv a license to display the preprint in perpetuity. It is made available under aCC-BY 4.0 International license.

277

278 Butyrate promotes mucin production

279 GCs specialise in producing and secreting mucin glycoproteins and other factors to form
280 a protective mucus layer in the intestine. We assessed their function according to the number
281 of GCs (normalised as the GC number per 200 enterocytes) and by mRNA expression of three
282 GC products in the ileum. GC numbers tended to be higher in the PN group compared with
283 controls, but the difference was not statistically significant (53.2±5 vs 44±9.4, p=0.08). The
284 addition of butyrate resulted in a further increase in abundance (63.6±8.5, $p<0.01$ vs controls,
285 $p<0.05$ vs PN). Expression of *Muc2*, the main secretory mucin, increased in the PN group
286 compared with controls, and was further potentiated by butyrate. *Muc3*, the dominant
287 transmembrane mucin, was elevated only in the PN+But group. *Fcgbp* expression was not
288 affected in any group (Fig 3). These data indicate that in response to the absence of enteral
289 feeding GCs increase activity, and that butyrate supplementation significantly stimulates this
290 process.

291 **Fig 3. mRNA expression of mucosa-forming genes in the ileum**. A: Muc2; B Muc3; C:
292 Fcgbp. mRNA expression is given as a fold change over the control group. Results are
293 presented using Tukey box-and-whisker plots as quartiles (25%, median, and 75%). $^{*}p<0.05$
294 PN vs control; $^{\dagger\dagger}p<0.01$ PN+But vs control; $^{\#}p<0.05$; $^{\#\#}p<0.01$ PN+But vs PN.

295

296 Butyrate alleviates PN-induced small intestinal permeability

297 The effect of butyrate on small intestinal integrity was assessed by *in vitro* permeability
298 for HRP and by the expression of tight junction proteins. Ileal segments of both the PN and
299 PN+But groups were more permeable for HRP compared with controls (Fig 4A). Butyrate
300 supplementation decreased intestinal permeability compared with the PN group, although it
301 did not match the control level. The expression of tight junction proteins (*ZO-1, claudin-7, E-*

bioRxiv preprint doi: https://doi.org/10.1101/443978; this version posted October 15, 2018. The copyright holder for this preprint (which was not certified by peer review) is the author/funder, who has granted bioRxiv a license to display the preprint in perpetuity. It is made available under aCC-BY 4.0 International license.

cadherin) was similar in the control and PN groups and significantly increased in the PN+But group (Figs 4B-D). In summary, these findings support the hypothesis that butyrate alleviates the detrimental effect of PN on intestinal permeability via the stimulation of tight junction protein expression.

Fig 4. The effect of butyrate on tight junction proteins mRNA expression and intestinal permeability. A: *ZO-1* mRNA; B *E-cadherin* mRNA; C *claudin-7* mRNA; D: HRP leakage *in vitro*. mRNA expression is given as a fold change over the control group. Results are presented using Tukey box-and-whisker plots as quartiles (25%, median, and 75%). $^{*}p<0.05$ PN vs control; $^{\dagger\dagger}p<0.01$ PN+But vs control; $^{\#}p<0.05$; $^{\#\#}p<0.01$ PN+But vs PN.

The effect of butyrate on lymphocyte phenotypes and cytokine expression

In order to determine the effect of butyrate on gut-associated T-cell subpopulations, we isolated lymphocytes from MLN and analysed them by flow cytometry (Fig 5). In MLN, PN alone did not affect the total number of CD4+ or CD8+ lymphocytes, CD4+/CD8+ ratio (2.3±0.5 vs 2.4±0.4) or percentage of different CD8+ subpopulations, but it did increase the percentage of CD4+Foxp3+CD25+ (Treg). Butyrate supplementation led to a significant rise in CD4+ lymphocytes but did not change the total number of CD8+ lymphocytes, resulting in an increased CD4+/CD8+ ratio (3.5±0.2).

Fig 5. The effect of butyrate on the distribution of T-cell subpopulations in mesenteric lymph nodes. A: Total CD4+ and CD8+ lymphocyte numbers; B: Tregs subpopulation. Results are presented using Tukey box-and-whisker plots as quartiles (25%, median, and 75%). $^{**}p<0.01$ PN vs control; $^{\dagger\dagger}p<0.05$ PN+But vs control; $^{\#\#}p<0.01$ PN+But vs PN.

bioRxiv preprint doi: https://doi.org/10.1101/443978; this version posted October 15, 2018. The copyright holder for this preprint (which was not certified by peer review) is the author/funder, who has granted bioRxiv a license to display the preprint in perpetuity. It is made available under aCC-BY 4.0 International license.

In the PN group, we found significant attenuation of IL-10 (Fig 6A) and IL-4 mRNA (Fig 6B) expression in Peyer's patches as well as IgA mRNA expression (Fig 6C) in the intestinal mucosa. In the PN+But group, the expression of both cytokines increased to the levels observed in controls and IgA expression was nearly normalised. Taken together, butyrate added to a PN mixture is associated with an increase in the total CD4+ lymphocyte population, normalisation of the Tregs subpopulation in MLN, and an increase in gut mucosal immunity.

Fig 6. The effect of butyrate on cytokine and IgA mRNA expression. A: IL-10 expression in Peyer's patches; B: IL-4 expression in Peyer's patches; C: IgA expression in the intestinal mucosa. mRNA expression is expressed as a fold change over the control group. Results are presented using Tukey box-and-whisker plots as quartiles (25%, median, and 75%). $^{*}p<0.05$, $^{***}p<0.001$ PN vs control; $^{\#}p<0.05$; $^{\#\#}p<0.01$ PN+But vs PN.

The effect of butyrate supplementation on the microbiota

Microbiota composition was assessed via sequencing of the 16S rRNA gene in caecum content sampled at the time of sacrifice. Alpha diversity was assessed in terms of species richness (OTU numbers, Chao1 index) or evenness (Shannon index, Simpson index) (Table 2). Caecal microbiota in PN+But group tend to be less diverse compared with control or PN groups but this tendency reached the statistical significance only when OTUs number is concerned.

Table 2. Alpha diversity.

	OTUs	Chao1	shannon	simpson
control	477 (180)	814 (340)	6.23 (1.14)	0.96 (0.03)
PN	429 (109)	726 (289)	6.04 (1.43)	0.96 (0.1)
PN+But	328 (157)†	583 (288)	4.53 (3.44)	0.85 (0.34)

Data are given as median and IQR. † $p<0.05$ PN+But vs control

bioRxiv preprint doi: https://doi.org/10.1101/443978; this version posted October 15, 2018. The copyright holder for this preprint (which was not certified by peer review) is the author/funder, who has granted bioRxiv a license to display the preprint in perpetuity. It is made available under aCC-BY 4.0 International license.

The absence of enteral feeding in combination with PN administration had a significant effect on gut microbiota composition. At the phylum level, *Proteobacteria* significantly increased in both PN-dependent groups. Butyrate administration was associated with a decrease in *Proteobacteria* abundance but this trend did not reached statistical significance. Butyrate supplementation counteracted the deregulation of *Cyanobacteria* observed in the PN group (Fig 7).

Fig 7. Microbiota composition in the caecum: phylum level. Results are presented using Tukey box-and-whisker plots as quartiles (25%, median, and 75%) and outliers (open circles). $^{*}p<0.05$, $^{***}p<0.001$ PN vs control; $^{\dagger\dagger}p<0.05$ PN+But vs control; $^{\#}p<0.05$ PN+But vs PN.

The distribution pattern of abundant (<1%) bacterial families is shown in Fig 8. *Porphyromonadaceae* and *Alcaligenaceae* were significantly elevated while the *Clostridiales vadinBB60* was reduced in both PN-dependent groups compared with controls. The abundance of *Bacteroidaceae, Enterobacteriaceae, Lachnospiraceae,* and *Lactobacillaceae* was significantly altered only in one of the PN-dependent groups compared with controls but the trend was similar, i.e. of the same orientation, in both of them. Butyrate supplementation had significant effect on the abundance of *Peptococcaceae* and one unidentified taxon belonging to *Gastranaerophilales*.

Fig 8. Distribution pattern of all abundant (<1%) bacterial families in the caecum. Lines show the fold change vs controls, green line represents the null change (controls vs controls). Bar charts demonstrate the relative abundance (%) of each family. Colour key: green = controls; black = PN; red = PN+But. The significance ($p<0.05$) is shown using coloured boxes above the family names.

bioRxiv preprint doi: https://doi.org/10.1101/443978; this version posted October 15, 2018. The copyright holder for this preprint (which was not certified by peer review) is the author/funder, who has granted bioRxiv a license to display the preprint in perpetuity. It is made available under aCC-BY 4.0 International license.

We identified 20 genera that were significantly differently ($p < 0.05$) represented in at least on of the PN-dependent group compared with controls (Fig 9). Five genera were deregulated in both the PN and PN+But groups, i.e. *Bacteroides, Parabacteroides, Alistipes, Parasutterella* (increased) and *Prevotellaceae NK4A214 group* (decreased). Compared with the PN group, butyrate supplementation resulted in the increased abundance of *Anaerostipes, Lachnospiraceae AC2044 group* and *Roseburia*, but decreased the representation of the *Prevotellaceae Ga6A1 group* and unidentified bacteria from the *Gastranaerophilales* order. Similar trend (PN+But < PN) was observed in case of *Desulfovibrio sp.* ($p=0.055$). All relevant statistical data are shown in Table S2. Our data confirm the profound effect of the lack of enteral feeding on microbiota composition. Butyrate supplementation counteracted only some of the alterations.

Fig 9. Heat map showing the fold change (A) and the abundance (%) (B) of genera that were differently ($p<0.05$) represented in at least two groups. Positive values correspond with an increase and negative values with a decrease in the first group compared with the second group. Shades of blue represents fold change decrease while shades of brown represent fold change increase. Uncoloured fields are not significant at $p<0.05$.

Discussion

Butyrate and non-immune defence systems

In the intestine, the basic line of defence (independent of immune cells) consists of a tight attachment of epithelial cells mediated by tight junction proteins, a mucin layer secreted by GCs, host defence peptides produced by Paneth cells, and enterocyte products like RegIIIγ and Muc3. All of these factors prevent bacteria from coming into contact with the sub-epithelial layer and thus inducing the inflammatory response. PN administration disturbs these systems (6, 7, 10, 30-33), resulting in the increased exposure of antigens to the immune

bioRxiv preprint doi: https://doi.org/10.1101/443978; this version posted October 15, 2018. The copyright holder for this preprint (which was not certified by peer review) is the author/funder, who has granted bioRxiv a license to display the preprint in perpetuity. It is made available under aCC-BY 4.0 International license.

system, increased intestinal permeability, and the establishment of pro-inflammatory status in the intestine.

Although there is abundant evidence (obtained both *in vitro* and *in vivo*) that butyrate affects all components of this defence system, the mechanism is not yet fully understood and controversies remain. Muc 2, secreted by GCs, is the major structural component of the intestinal mucus. Muc 3 is a transmembrane mucin produced by enterocytes and the major component of glycocalyx, which plays an active role in the intestinal mucosal defence (34). Studies published thus far have only focused on the effect of butyrate on mucin production when administered per rectum or in cell lines *in vitro*; furthermore, these results are rather inconsistent (35, 36). Gaudier (37) reported that, *in vitro,* butyrate grossly stimulated Muc2 expression but only in a glucose-deprived medium, while the effect of butyrate was dose-dependent and inhibitory at higher concentrations. These findings indicate that the effect of butyrate on mucus formation is context-dependent. The stimulatory effect of butyrate on host defence peptides and tight junction protein expression has been proved both *in vitro* and after dietary supplementation *in vivo* (38-42). Nevertheless, to our knowledge, no study has evaluated the effect of butyrate administered parenterally. Our data show that supplementation of a PN mixture with butyrate at a concentration within physiological limits (9 mM) upregulates the expression of all components of the non-immune defence – including mucins, host defence peptides and tight junction proteins in the ileum – while also improving intestinal permeability. We conclude that enforcement of the intestinal barrier may represent one of the beneficial effects of i.v. butyrate in the context of total dependence on PN and the absence of enteral nutrition and/or butyrate producers.

Butyrate and immune functions

bioRxiv preprint doi: https://doi.org/10.1101/443978; this version posted October 15, 2018. The copyright holder for this preprint (which was not certified by peer review) is the author/funder, who has granted bioRxiv a license to display the preprint in perpetuity. It is made available under aCC-BY 4.0 International license.

Total dependence on PN in critically ill patients is accompanied by decreased immune responsiveness, reduced gut-associated lymphoid tissue (GALT) mass, diminished IgA secretion, and increased risk of generalised sepsis (43). Nevertheless, it seems that the main factor responsible for immune dysfunction in PN-dependent patients is not PN administration itself, but the lack of enteral feeding (1). One consequence of the absence of enterally provided nutrients is low SCFA content in the gut. SCFA and, in particular, butyrate have been shown to influence immune cells towards anti-inflammatory and tolerogenic phenotypes (44) and to induce the differentiation of Foxp3+ Treg lymphocytes (45). In mice, an SCFA mixture administered *per os* increased the numbers of IgA-secreting lamina propria B cells, IgA expression or levels of secreted IgA in various compartments of the intestine, and IgA and IgG levels in the blood circulation (46). To our knowledge, only one study has focused on the effect of butyrate when added to PN on GALT. In mice, butyrate partially restored a PN-induced drop in lymphocyte numbers in Peyer's patches and intestinal IgA levels (47). In our study, butyrate supplementation was associated with an increase in CD4+ lymphocyte numbers, and an increase in the CD4+/CD8+ ratio in MLN. Rather surprisingly, we observed an increase of Tregs in MLN of rats administered a PN mixture without butyrate, while the addition of butyrate resulted in a decrease in Tregs percentage to the control level. Treg cells expressing transcription factor Foxp3 are believed to play a key role in limiting inflammatory responses in the intestine (48), as they inhibit bystander T-cell activation either by a contact-dependent mechanism or through soluble factors (49). Paradoxically, $Foxp3^+$ Tregs are more common in the inflamed intestinal mucosa of IBD patients, leading to a reciprocal drop in circulating Treg frequency in the peripheral blood; this likely reflects sequestration of these cells to the site of inflammation (50, 51). In a rat sepsis model, the pro-survival treatment was associated with a decrease in spleen Tregs (52) and in septic patients the persistence of elevated Treg indicated poor outcomes (53). We hypothesise that in our experimental setting

bioRxiv preprint doi: https://doi.org/10.1101/443978; this version posted October 15, 2018. The copyright holder for this preprint (which was not certified by peer review) is the author/funder, who has granted bioRxiv a license to display the preprint in perpetuity. It is made available under aCC-BY 4.0 International license.

447 decreased Treg frequency in MLN in the PN+But group reflects the lower inflammatory
448 status of the intestinal epithelium, thus reducing the need to produce an anti-inflammatory
449 response.

450 IgA production by plasmatic B cells in the submucosal layer is regulated by Th1 and
451 Th2 cytokines produced by different T-helper subpopulations. While Th1 cytokines (IFNγ)
452 downregulate IgA production, Th2 cytokines (IL-4, IL-5, IL-6, and IL-10) stimulate it (54).
453 Hanna (55) reported that PN depressed both IL-4 and IL-10 levels in small intestine
454 homogenates but that IFNγ levels remained unchanged, resulting in an imbalance between
455 pro-/anti-IgA-regulating cytokines and a subsequent reduction in IgA production. Our data
456 confirm this observation concerning the effect of non-supplemented PN. Butyrate
457 supplementation resulted in increases in IL-4 and IL-10 expression to control levels and the
458 near normalisation of IgA expression. These data suggest that intraepithelial Th2 helpers are
459 one of the targets of butyrate and that butyrate supplementation may restore the PN-induced
460 cytokine imbalance.

461

462 ## Butyrate and the microbiota

463 The gut microbiome in animal models of PN is characterised by a significant shift in
464 microbiota composition, particularly a loss of *Firmicutes* and an enrichment of *Bacteroidetes*
465 and *Proteobacteria* (3, 7). In our study, we observed a shift towards an unfavourable
466 microbiota composition, particularly an enrichment of *Proteobacteria* and the reduction of
467 bacteria involved in butyrate production (*Lactobacillaceae* or *Lachnospiraceae*) in both PN-
468 dependent groups. While the abundance of butyrate producers was not affected by butyrate
469 supplementation we observed a trend, albeit not statistically significant, towards
470 *Proteobacteria* reduction in butyrate-administered animals. Interestingly, butyrate

bioRxiv preprint doi: https://doi.org/10.1101/443978; this version posted October 15, 2018. The copyright holder for this preprint (which was not certified by peer review) is the author/funder, who has granted bioRxiv a license to display the preprint in perpetuity. It is made available under aCC-BY 4.0 International license.

supplementation (but not enteral deprivation/PN administration alone) was associated with a tendency to the loss of diversity.

Although the effects of dietary fibre on the gut microbiota have been described elsewhere (56), information concerning the direct effect of butyrate on the gut microbiota is scarce. Dietary butyrate was reported to reduce coliform bacteria (57) and to increase the abundance of *Lactobacillus* (42, 58) and butyrate producers *Blautia* and *Anaerostipes* (42). We observed no radical effect of *i.v.* butyrate, as it did not attenuate deregulation of the main contributors to PN-induced dysbiosis. Nevertheless, butyrate supplementation has been associated with an increased abundance of several potentially beneficial genera (*Anaerostipes, Roseburia, Lachnospiraceae AC2044 group*), a decreased abundance in the opportunistic human pathogen *Desulfovibrio* (59) and a trend towards attenuation in *Proteobacteria* dominance. We suggest that this subtle shift in microbiota composition may contribute, along with other mechanisms, to the overall beneficial effect of butyrate.

Conclusion

We report that supplementation of a PN mixture with butyrate resulted in a significant enhancement of gut defence systems, i.e. increased expression of mucins, tight junction proteins and host defence peptides, and improvement of PN-induced aggravation of intestinal permeability. Lack of enteral nutrition and/or PN administration led to a shift in caecal microbiota composition. Although butyrate did not reverse the altered expression of most taxa, it did influence the abundance of several potentially beneficial or pathogenic genera what might contribute to its overall advantageous effect. We conclude that supplementation of a PN mixture with butyrate may represent a prospective therapeutic approach for mitigating the adverse effects of parenteral nutrition.

bioRxiv preprint doi: https://doi.org/10.1101/443978; this version posted October 15, 2018. The copyright holder for this preprint (which was not certified by peer review) is the author/funder, who has granted bioRxiv a license to display the preprint in perpetuity. It is made available under aCC-BY 4.0 International license.

Supporting information

Table S1. Composition of parenteral nutrition mixture

Table S2. Statistical analysis of sequencing data

Author Contributions

Conceptualization: Monika Cahova

Data curation: Petra Videnska, Zuzana Jirsova, Monika Cahova

Funding acquisition: Monika Cahova

Investigation: Zuzana Jirsova, Marie Heczkova, Helena Dankova, Hana Vespalcova, Lenka Micenkova, Lenka Bartonova, Alena Lodererova, Alena Sekerkova

Validation: Lucia Prefertusová, Hana Malinska Eva Sticova, Petra Videnska

Visualization: Helena Dankova, Hana Vespalcova,

Writing ± original draft: Zuzana Jirsova, Petra Videnska, Marie Heczkova, Monika Cahova

Writing ± review & editing: Zuzana Jirsova, Petra Videnska, Monika Cahova

References

1. Wildhaber BE, Yang H, Spencer AU, Drongowski RA, Teitelbaum DH. Lack of enteral nutrition--effects on the intestinal immune system. J Surg Res. 2005;123(1):8-16.

2. Alverdy JC, Aoys E, Moss GS. Total parenteral nutrition promotes bacterial translocation from the gut. Surgery. 1988;104(2):185-90.

3. Hodin CM, Visschers RG, Rensen SS, Boonen B, Olde Damink SW, Lenaerts K, et al. Total parenteral nutrition induces a shift in the Firmicutes to Bacteroidetes ratio in association with Paneth cell activation in rats. J Nutr. 2012;142(12):2141-7.

4. Iida T, Onodera K, Nakase H. Role of autophagy in the pathogenesis of inflammatory bowel disease. World J Gastroenterol. 2017;23(11):1944-53.

5. Hodin CM, Lenaerts K, Grootjans J, de Haan JJ, Hadfoune M, Verheyen FK, et al. Starvation compromises Paneth cells. Am J Pathol. 2011;179(6):2885-93.

bioRxiv preprint doi: https://doi.org/10.1101/443978; this version posted October 15, 2018. The copyright holder for this preprint (which was not certified by peer review) is the author/funder, who has granted bioRxiv a license to display the preprint in perpetuity. It is made available under aCC-BY 4.0 International license.

523 6. Pierre JF, Heneghan AF, Tsao FH, Sano Y, Jonker MA, Omata J, et al. Route and type
524 of nutrition and surgical stress influence secretory phospholipase A2 secretion of the murine
525 small intestine. JPEN J Parenter Enteral Nutr. 2011;35(6):748-56.
526 7. Heneghan AF, Pierre JF, Tandee K, Shanmuganayagam D, Wang X, Reed JD, et al.
527 Parenteral nutrition decreases paneth cell function and intestinal bactericidal activity while
528 increasing susceptibility to bacterial enteroinvasion. JPEN J Parenter Enteral Nutr.
529 2014;38(7):817-24.
530 8. Adler KB, Tuvim MJ, Dickey BF. Regulated mucin secretion from airway epithelial
531 cells. Front Endocrinol (Lausanne). 2013;4:129.
532 9. Allaire JM, Morampudi V, Crowley SM, Stahl M, Yu H, Bhullar K, et al. Frontline
533 defenders: goblet cell mediators dictate host-microbe interactions in the intestinal tract during
534 health and disease. Am J Physiol Gastrointest Liver Physiol. 2018;314(3):G360-G77.
535 10. Conour JE, Ganessunker D, Tappenden KA, Donovan SM, Gaskins HR. Acidomucin
536 goblet cell expansion induced by parenteral nutrition in the small intestine of piglets. Am J
537 Physiol Gastrointest Liver Physiol. 2002;283(5):G1185-96.
538 11. Smirnov A, Sklan D, Uni Z. Mucin dynamics in the chick small intestine are altered
539 by starvation. J Nutr. 2004;134(4):736-42.
540 12. Zhou Q, Cadrin M, Herrmann H, Chen CH, Chalkley RJ, Burlingame AL, et al.
541 Keratin 20 serine 13 phosphorylation is a stress and intestinal goblet cell marker. J Biol
542 Chem. 2006;281(24):16453-61.
543 13. Mazmanian SK, Liu CH, Tzianabos AO, Kasper DL. An immunomodulatory molecule
544 of symbiotic bacteria directs maturation of the host immune system. Cell. 2005;122(1):107-
545 18.

bioRxiv preprint doi: https://doi.org/10.1101/443978; this version posted October 15, 2018. The copyright holder for this preprint (which was not certified by peer review) is the author/funder, who has granted bioRxiv a license to display the preprint in perpetuity. It is made available under aCC-BY 4.0 International license.

546 14. Christensen HR, Frokiaer H, Pestka JJ. Lactobacilli differentially modulate expression
547 of cytokines and maturation surface markers in murine dendritic cells. J Immunol.
548 2002;168(1):171-8.
549 15. Ivanov, II, Frutos Rde L, Manel N, Yoshinaga K, Rifkin DB, Sartor RB, et al. Specific
550 microbiota direct the differentiation of IL-17-producing T-helper cells in the mucosa of the
551 small intestine. Cell Host Microbe. 2008;4(4):337-49.
552 16. Iwasaki A, Kelsall BL. Freshly isolated Peyer's patch, but not spleen, dendritic cells
553 produce interleukin 10 and induce the differentiation of T helper type 2 cells. J Exp Med.
554 1999;190(2):229-39.
555 17. Kelsall BL, Leon F. Involvement of intestinal dendritic cells in oral tolerance,
556 immunity to pathogens, and inflammatory bowel disease. Immunol Rev. 2005;206:132-48.
557 18. Kelly D, Campbell JI, King TP, Grant G, Jansson EA, Coutts AG, et al. Commensal
558 anaerobic gut bacteria attenuate inflammation by regulating nuclear-cytoplasmic shuttling of
559 PPAR-gamma and RelA. Nat Immunol. 2004;5(1):104-12.
560 19. Lee J, Mo JH, Katakura K, Alkalay I, Rucker AN, Liu YT, et al. Maintenance of
561 colonic homeostasis by distinctive apical TLR9 signalling in intestinal epithelial cells. Nat
562 Cell Biol. 2006;8(12):1327-36.
563 20. Beutler B, Rietschel ET. Innate immune sensing and its roots: the story of endotoxin.
564 Nat Rev Immunol. 2003;3(2):169-76.
565 21. Demehri FR, Barrett M, Teitelbaum DH. Changes to the Intestinal Microbiome With
566 Parenteral Nutrition: Review of a Murine Model and Potential Clinical Implications. Nutr
567 Clin Pract. 2015;30(6):798-806.
568 22. Miyasaka EA, Feng Y, Poroyko V, Falkowski NR, Erb-Downward J, Gillilland MG,
569 3rd, et al. Total parenteral nutrition-associated lamina propria inflammation in mice is
570 mediated by a MyD88-dependent mechanism. J Immunol. 2013;190(12):6607-15.

bioRxiv preprint doi: https://doi.org/10.1101/443978; this version posted October 15, 2018. The copyright holder for this preprint (which was not certified by peer review) is the author/funder, who has granted bioRxiv a license to display the preprint in perpetuity. It is made available under aCC-BY 4.0 International license.

571 23. Guilloteau P, Martin L, Eeckhaut V, Ducatelle R, Zabielski R, Van Immerseel F. From
572 the gut to the peripheral tissues: the multiple effects of butyrate. Nutr Res Rev.
573 2010;23(2):366-84.
574 24. Apprill A, McNally S, Parsons R, Weber L. Minor revision to V4 region SSU rRNA
575 806R gene primer greatly increases detection of SAR11 bacterioplankton. Aquat Microb Ecol.
576 2015;75(2):129-37.
577 25. Caporaso JG, Lauber CL, Walters WA, Berg-Lyons D, Lozupone CA, Turnbaugh PJ,
578 et al. Global patterns of 16S rRNA diversity at a depth of millions of sequences per sample.
579 Proc Natl Acad Sci U S A. 2011;108 Suppl 1:4516-22.
580 26. Caporaso JG, Kuczynski J, Stombaugh J, Bittinger K, Bushman FD, Costello EK, et
581 al. QIIME allows analysis of high-throughput community sequencing data. Nat Methods.
582 2010;7(5):335-6.
583 27. Edgar RC. Search and clustering orders of magnitude faster than BLAST.
584 Bioinformatics. 2010;26(19):2460-1.
585 28. Aitchison J. The Statistical Analysis of Compositional Data (Monographs on Statistics
586 and Applied Probability). London: Chapman & Hall Ltd.; 1986. 416 p.
587 29. R Core Team (2017). R: A language and environment for statistical computing.
588 Vienna, Austria: R Foundation for Statistical Computing.
589 30. Busch RA, Heneghan AF, Pierre JF, Neuman JC, Reimer CA, Wang X, et al.
590 Bombesin Preserves Goblet Cell Resistin-Like Molecule beta During Parenteral Nutrition but
591 Not Other Goblet Cell Products. JPEN J Parenter Enteral Nutr. 2016;40(7):1042-9.
592 31. Wang J, Tian F, Zheng H, Tian H, Wang P, Zhang L, et al. N-3 polyunsaturated fatty
593 acid-enriched lipid emulsion improves Paneth cell function via the IL-22/Stat3 pathway in a
594 mouse model of total parenteral nutrition. Biochem Biophys Res Commun. 2017;490(2):253-
595 9.

bioRxiv preprint doi: https://doi.org/10.1101/443978; this version posted October 15, 2018. The copyright holder for this preprint (which was not certified by peer review) is the author/funder, who has granted bioRxiv a license to display the preprint in perpetuity. It is made available under aCC-BY 4.0 International license.

596 32. Omata J, Pierre JF, Heneghan AF, Tsao FH, Sano Y, Jonker MA, et al. Parenteral
597 nutrition suppresses the bactericidal response of the small intestine. Surgery. 2013;153(1):17-
598 24.
599 33. Sun X, Yang H, Nose K, Nose S, Haxhija EQ, Koga H, et al. Decline in intestinal
600 mucosal IL-10 expression and decreased intestinal barrier function in a mouse model of total
601 parenteral nutrition. Am J Physiol Gastrointest Liver Physiol. 2008;294(1):G139-47.
602 34. Shekels LL, Ho SB. Characterization of the mouse Muc3 membrane bound intestinal
603 mucin 5' coding and promoter regions: regulation by inflammatory cytokines. Biochim
604 Biophys Acta. 2003;1627(2-3):90-100.
605 35. Hamer HM, Jonkers DM, Renes IB, Vanhoutvin SA, Kodde A, Troost FJ, et al.
606 Butyrate enemas do not affect human colonic MUC2 and TFF3 expression. Eur J
607 Gastroenterol Hepatol. 2010;22(9):1134-40.
608 36. Jiminez JA, Uwiera TC, Abbott DW, Uwiera RRE, Inglis GD. Butyrate
609 Supplementation at High Concentrations Alters Enteric Bacterial Communities and Reduces
610 Intestinal Inflammation in Mice Infected with Citrobacter rodentium. mSphere. 2017;2(4).
611 37. Gaudier E, Jarry A, Blottiere HM, de Coppet P, Buisine MP, Aubert JP, et al. Butyrate
612 specifically modulates MUC gene expression in intestinal epithelial goblet cells deprived of
613 glucose. Am J Physiol-Gastr L. 2004;287(6):G1168-G74.
614 38. Cresci GA, Glueck B, McMullen MR, Xin W, Allende D, Nagy LE. Prophylactic
615 tributyrin treatment mitigates chronic-binge ethanol-induced intestinal barrier and liver injury.
616 J Gastroenterol Hepatol. 2017;32(9):1587-97.
617 39. Dou X, Han J, Song W, Dong N, Xu X, Zhang W, et al. Sodium butyrate improves
618 porcine host defense peptide expression and relieves the inflammatory response upon Toll-
619 like receptor 2 activation and histone deacetylase inhibition in porcine kidney cells.
620 Oncotarget. 2017;8(16):26532-51.

bioRxiv preprint doi: https://doi.org/10.1101/443978; this version posted October 15, 2018. The copyright holder for this preprint (which was not certified by peer review) is the author/funder, who has granted bioRxiv a license to display the preprint in perpetuity. It is made available under aCC-BY 4.0 International license.

621 40. Sunkara LT, Achanta M, Schreiber NB, Bommineni YR, Dai G, Jiang W, et al.
622 Butyrate enhances disease resistance of chickens by inducing antimicrobial host defense
623 peptide gene expression. PLoS One. 2011;6(11):e27225.
624 41. Xiong H, Guo B, Gan Z, Song D, Lu Z, Yi H, et al. Butyrate upregulates endogenous
625 host defense peptides to enhance disease resistance in piglets via histone deacetylase
626 inhibition. Sci Rep. 2016;6:27070.
627 42. Zhou D, Pan Q, Xin FZ, Zhang RN, He CX, Chen GY, et al. Sodium butyrate
628 attenuates high-fat diet-induced steatohepatitis in mice by improving gut microbiota and
629 gastrointestinal barrier. World J Gastroenterol. 2017;23(1):60-75.
630 43. Pierre JF. Gastrointestinal immune and microbiome changes during parenteral
631 nutrition. Am J Physiol Gastrointest Liver Physiol. 2017;312(3):G246-G56.
632 44. Rooks MG, Garrett WS. Gut microbiota, metabolites and host immunity. Nat Rev
633 Immunol. 2016;16(6):341-52.
634 45. Arpaia N, Campbell C, Fan X, Dikiy S, van der Veeken J, deRoos P, et al. Metabolites
635 produced by commensal bacteria promote peripheral regulatory T-cell generation. Nature.
636 2013;504(7480):451-5.
637 46. Kim M, Qie Y, Park J, Kim CH. Gut Microbial Metabolites Fuel Host Antibody
638 Responses. Cell Host Microbe. 2016;20(2):202-14.
639 47. Murakoshi S, Fukatsu K, Omata J, Moriya T, Noguchi M, Saitoh D, et al. Effects of
640 adding butyric acid to PN on gut-associated lymphoid tissue and mucosal immunoglobulin A
641 levels. JPEN J Parenter Enteral Nutr. 2011;35(4):465-72.
642 48. Josefowicz SZ, Niec RE, Kim HY, Treuting P, Chinen T, Zheng Y, et al.
643 Extrathymically generated regulatory T cells control mucosal TH2 inflammation. Nature.
644 2012;482(7385):395-9.

bioRxiv preprint doi: https://doi.org/10.1101/443978; this version posted October 15, 2018. The copyright holder for this preprint (which was not certified by peer review) is the author/funder, who has granted bioRxiv a license to display the preprint in perpetuity. It is made available under aCC-BY 4.0 International license.

645 49. Lord JD. Promises and paradoxes of regulatory T cells in inflammatory bowel disease.
646 World J Gastroenterol. 2015;21(40):11236-45.
647 50. Maul J, Loddenkemper C, Mundt P, Berg E, Giese T, Stallmach A, et al. Peripheral
648 and intestinal regulatory CD4+ CD25(high) T cells in inflammatory bowel disease.
649 Gastroenterology. 2005;128(7):1868-78.
650 51. Lord JD, Valliant-Saunders K, Hahn H, Thirlby RC, Ziegler SF. Paradoxically
651 increased FOXP3+ T cells in IBD do not preferentially express the isoform of FOXP3 lacking
652 exon 2. Dig Dis Sci. 2012;57(11):2846-55.
653 52. Cao S, Ren J, Sun L, Gu G, Yuan Y, Li J. Fish oil-supplemented parenteral nutrition
654 prolongs survival while beneficially altering phospholipids' Fatty Acid composition and
655 modulating immune function in rat sepsis. Shock. 2011;36(2):184-90.
656 53. Venet F, Chung CS, Monneret G, Huang X, Horner B, Garber M, et al. Regulatory T
657 cell populations in sepsis and trauma. J Leukoc Biol. 2008;83(3):523-35.
658 54. Kramer DR, Sutherland RM, Bao S, Husband AJ. Cytokine mediated effects in
659 mucosal immunity. Immunol Cell Biol. 1995;73(5):389-96.
660 55. Hanna MK, Kudsk KA. Nutritional and pharmacological enhancement of gut-
661 associated lymphoid tissue. Can J Gastroenterol. 2000;14 Suppl D:145D-51D.
662 56. Whelan K. Mechanisms and effectiveness of prebiotics in modifying the
663 gastrointestinal microbiota for the management of digestive disorders. Proc Nutr Soc.
664 2013;72(3):288-98.
665 57. Galfi P, Bokori J. Feeding trial in pigs with a diet containing sodium n-butyrate. Acta
666 Vet Hung. 1990;38(1-2):3-17.
667 58. Jellbauer S, Raffatellu M. An intestinal arsonist: pathobiont ignites IBD and flees the
668 scene. Gut. 2014;63(7):1034-5.

bioRxiv preprint doi: https://doi.org/10.1101/443978; this version posted October 15, 2018. The copyright holder for this preprint (which was not certified by peer review) is the author/funder, who has granted bioRxiv a license to display the preprint in perpetuity. It is made available under aCC-BY 4.0 International license.

669 59. Verstreken I, Laleman W, Wauters G, Verhaegen J. Desulfovibrio desulfuricans
670 bacteremia in an immunocompromised host with a liver graft and ulcerative colitis. J Clin
671 Microbiol. 2012;50(1):199-201.

672

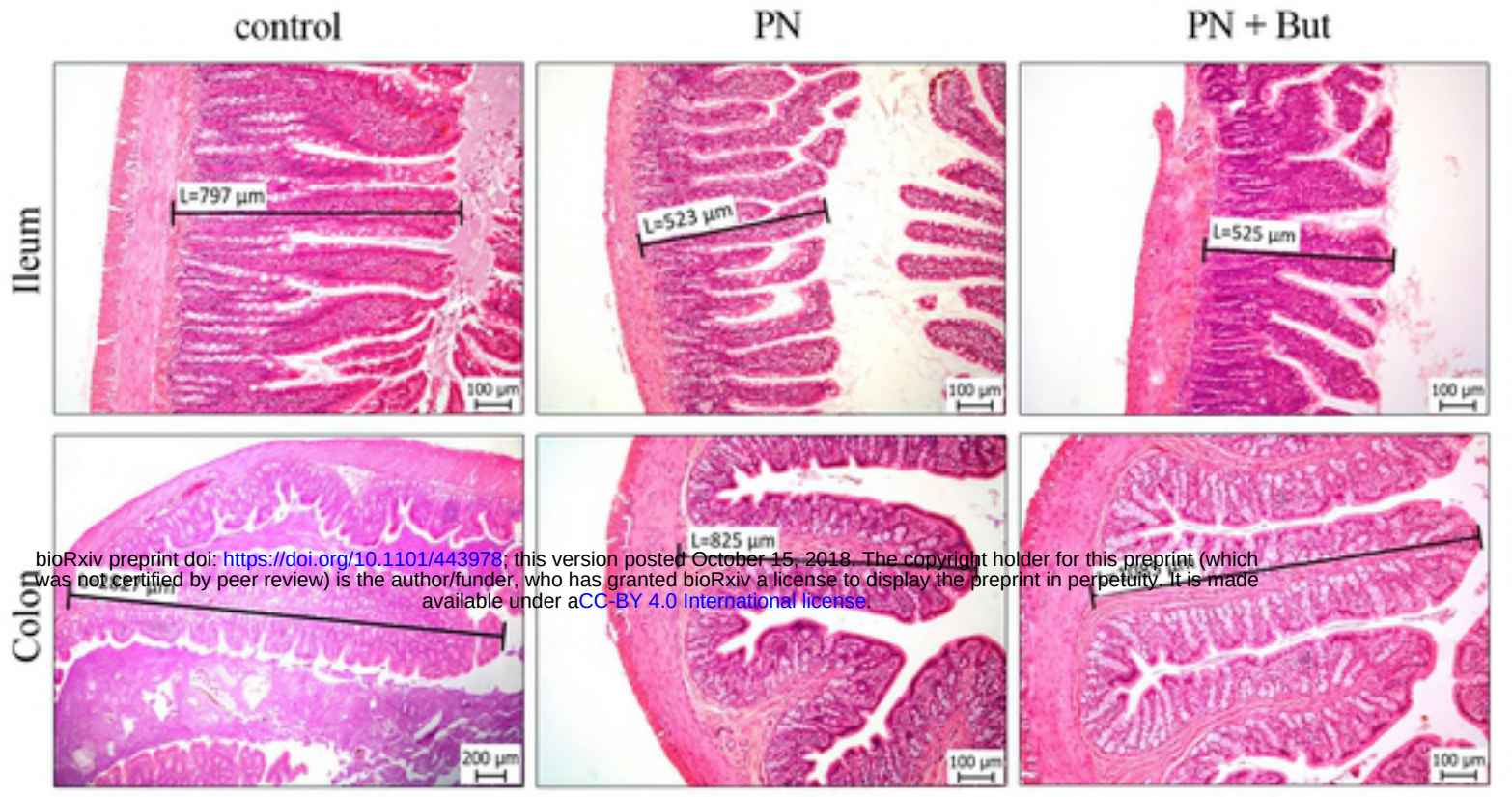

bioRxiv preprint doi: https://doi.org/10.1101/443978; this version posted October 15, 2018. The copyright holder for this preprint (which was not certified by peer review) is the author/funder, who has granted bioRxiv a license to display the preprint in perpetuity. It is made available under aCC-BY 4.0 International license.

Figure 1

bioRxiv preprint doi: https://doi.org/10.1101/443978; this version posted October 15, 2018. The copyright holder for this preprint (which was not certified by peer review) is the author/funder, who has granted bioRxiv a license to display the preprint in perpetuity. It is made available under aCC-BY 4.0 International license.

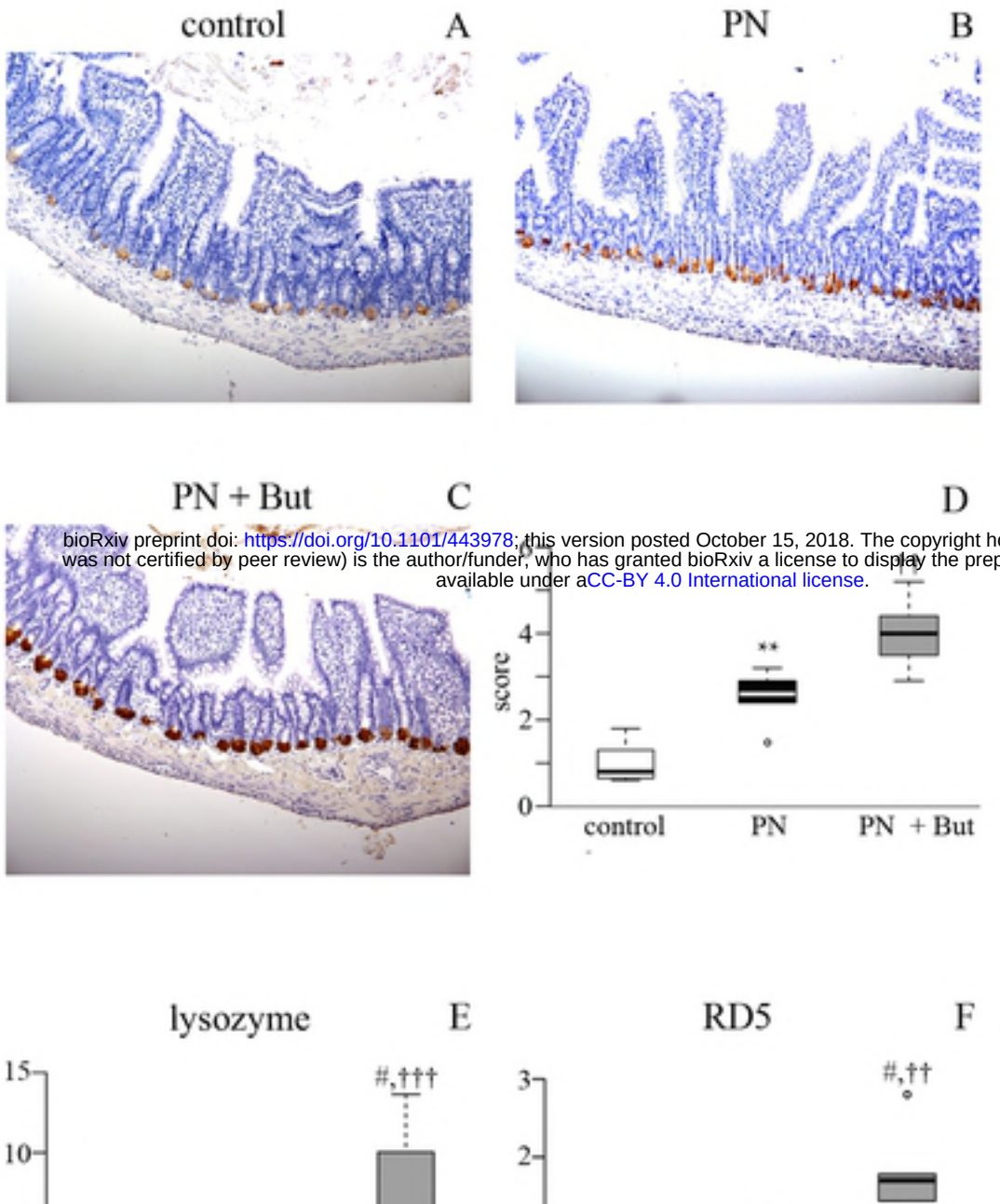

Figure 2

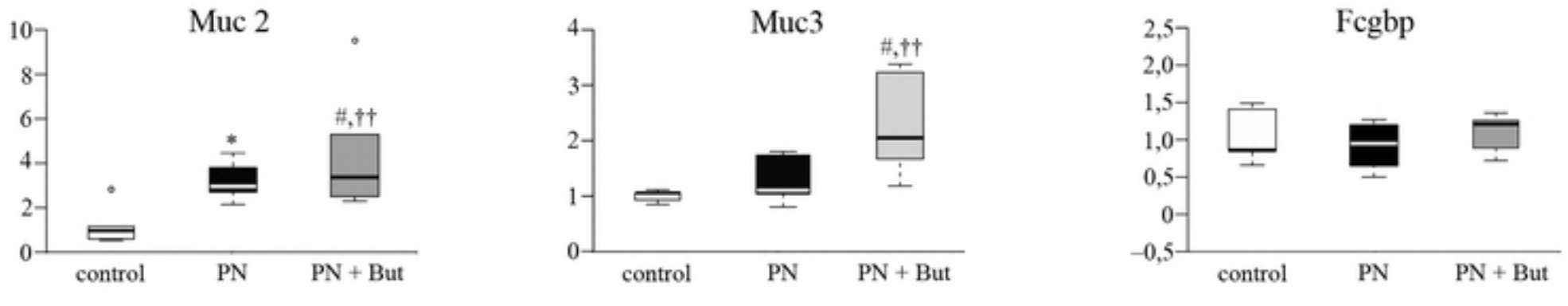

bioRxiv preprint doi: https://doi.org/10.1101/443978; this version posted October 15, 2018. The copyright holder for this preprint (which was not certified by peer review) is the author/funder, who has granted bioRxiv a license to display the preprint in perpetuity. It is made available under aCC-BY 4.0 International license.

Figure 3

bioRxiv preprint doi: https://doi.org/10.1101/443978; this version posted October 15, 2018. The copyright holder for this preprint (which was not certified by peer review) is the author/funder, who has granted bioRxiv a license to display the preprint in perpetuity. It is made available under aCC-BY 4.0 International license.

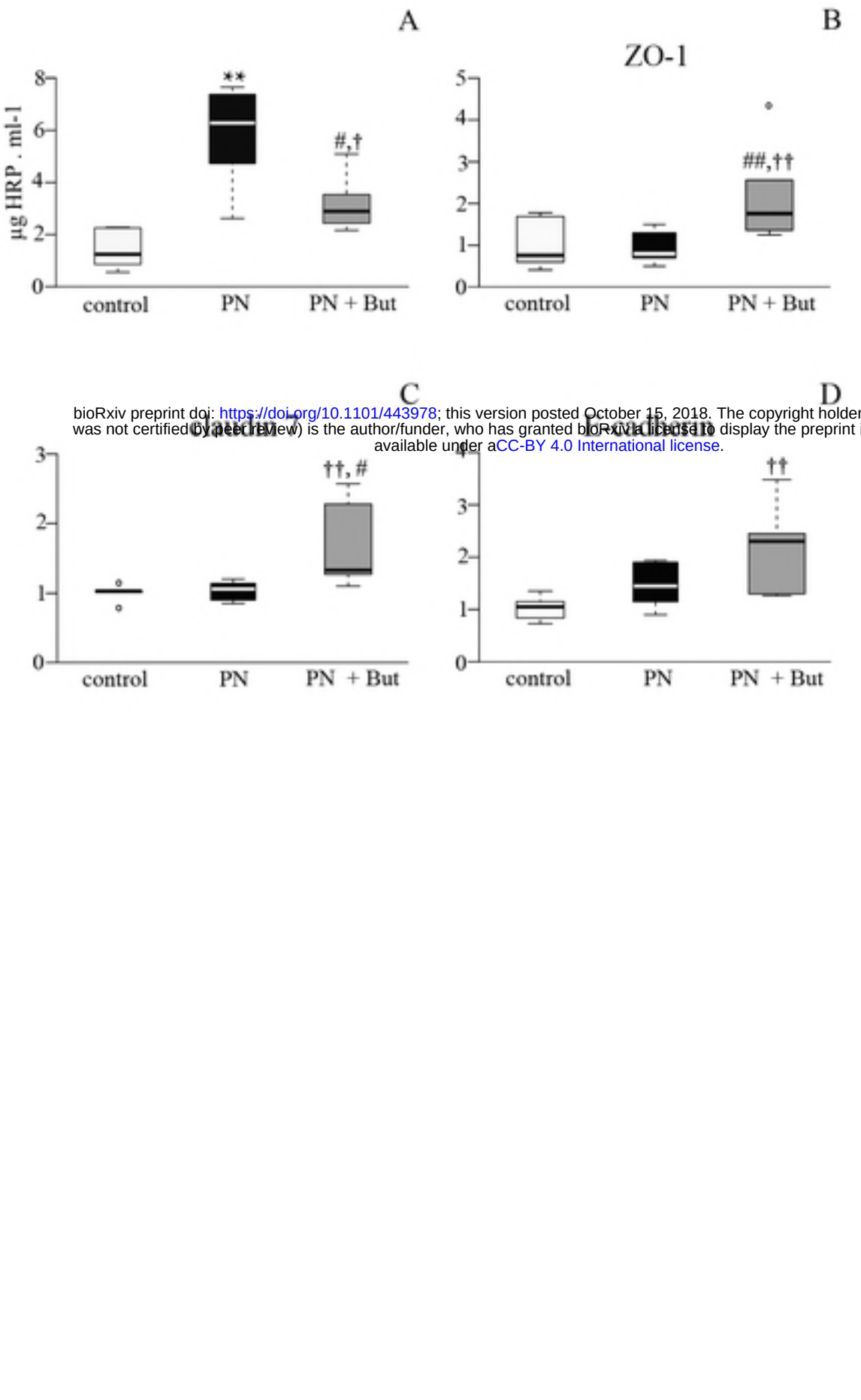

Figure 4

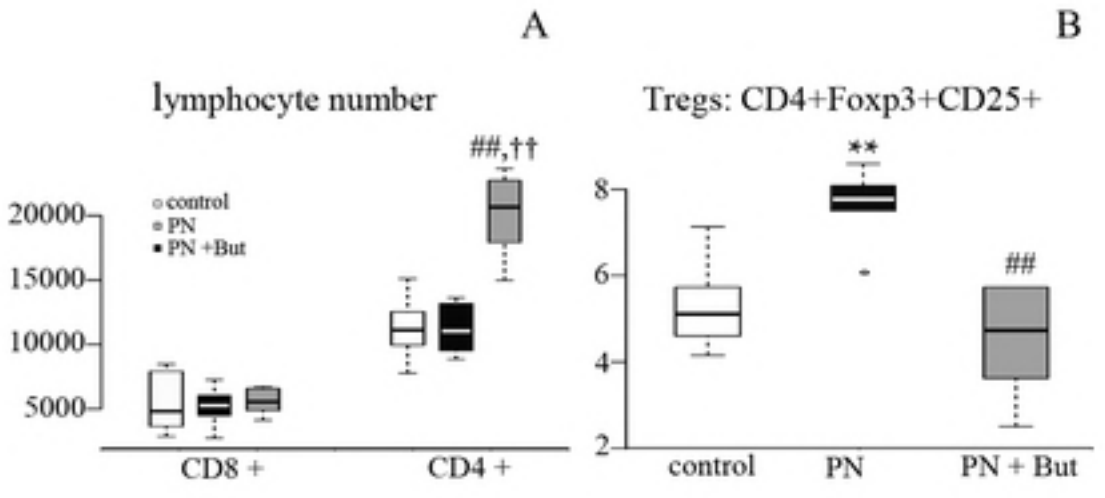

bioRxiv preprint doi: https://doi.org/10.1101/443978; this version posted October 15, 2018. The copyright holder for this preprint (which was not certified by peer review) is the author/funder, who has granted bioRxiv a license to display the preprint in perpetuity. It is made available under aCC-BY 4.0 International license.

Figure 5

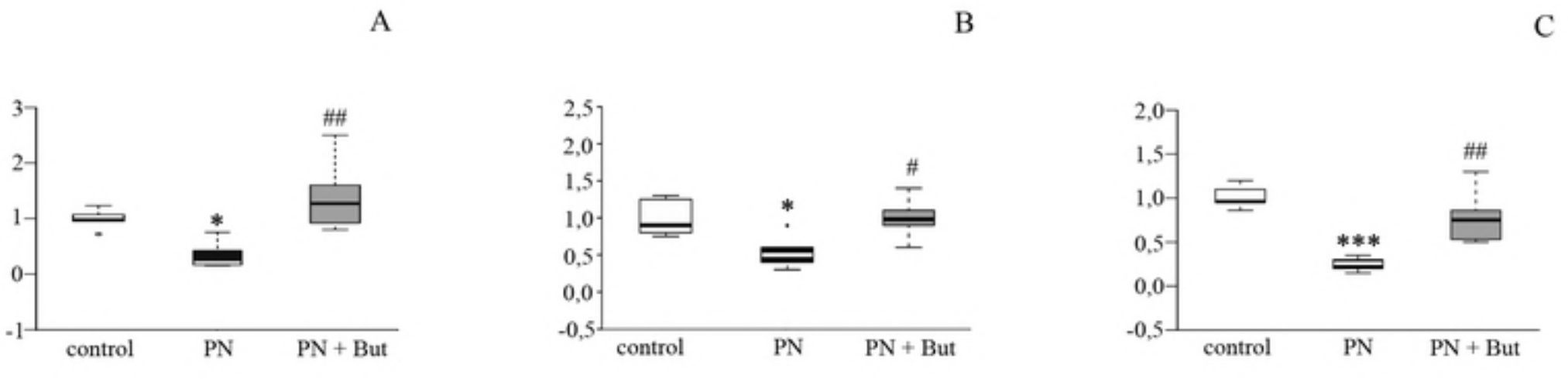

bioRxiv preprint doi: https://doi.org/10.1101/443978; this version posted October 15, 2018. The copyright holder for this preprint (which was not certified by peer review) is the author/funder, who has granted bioRxiv a license to display the preprint in perpetuity. It is made available under aCC-BY 4.0 International license.

Figure 6

bioRxiv preprint doi: https://doi.org/10.1101/443978; this version posted October 15, 2018. The copyright holder for this preprint (which was not certified by peer review) is the author/funder, who has granted bioRxiv a license to display the preprint in perpetuity. It is made available under aCC-BY 4.0 International license.

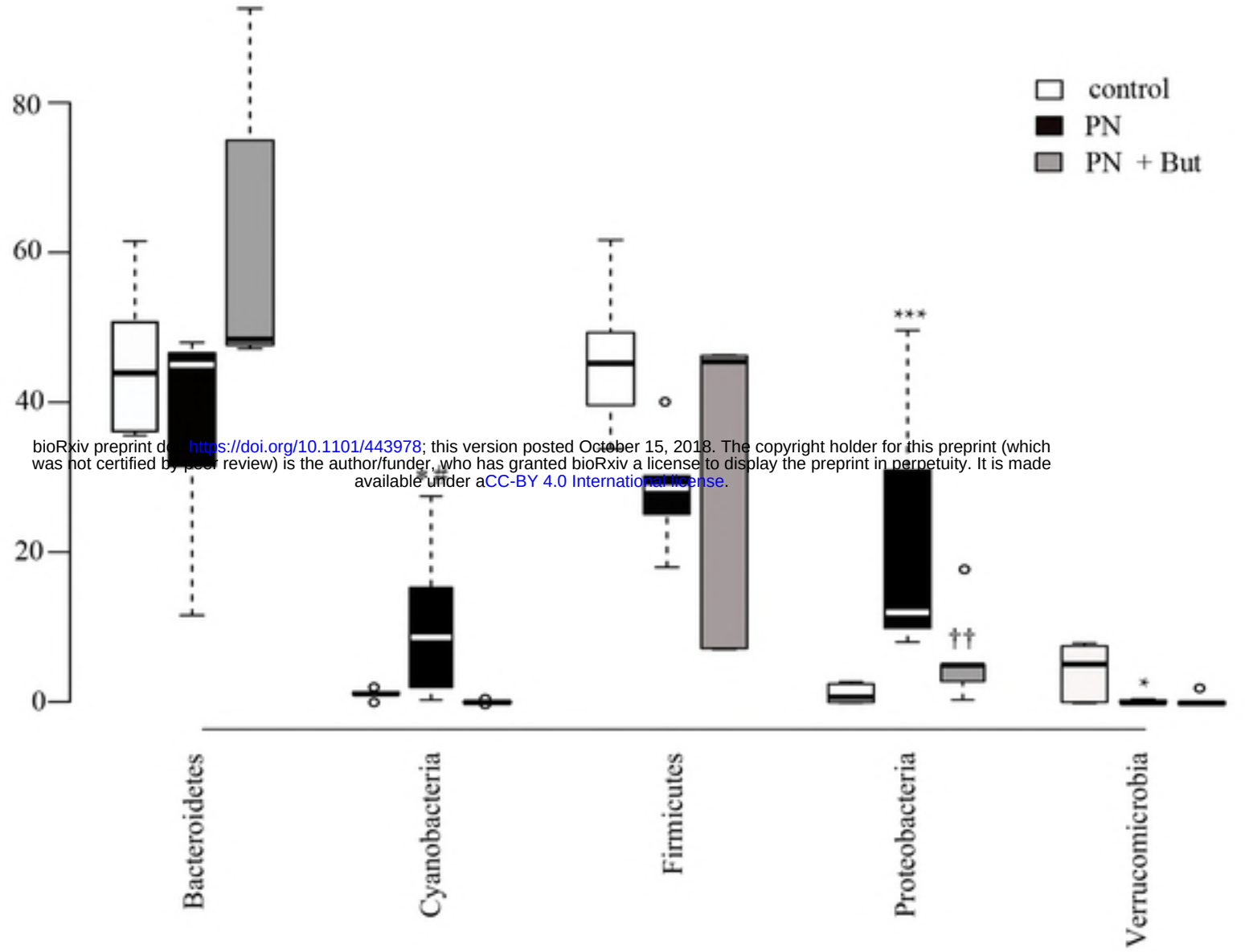

Figure 7

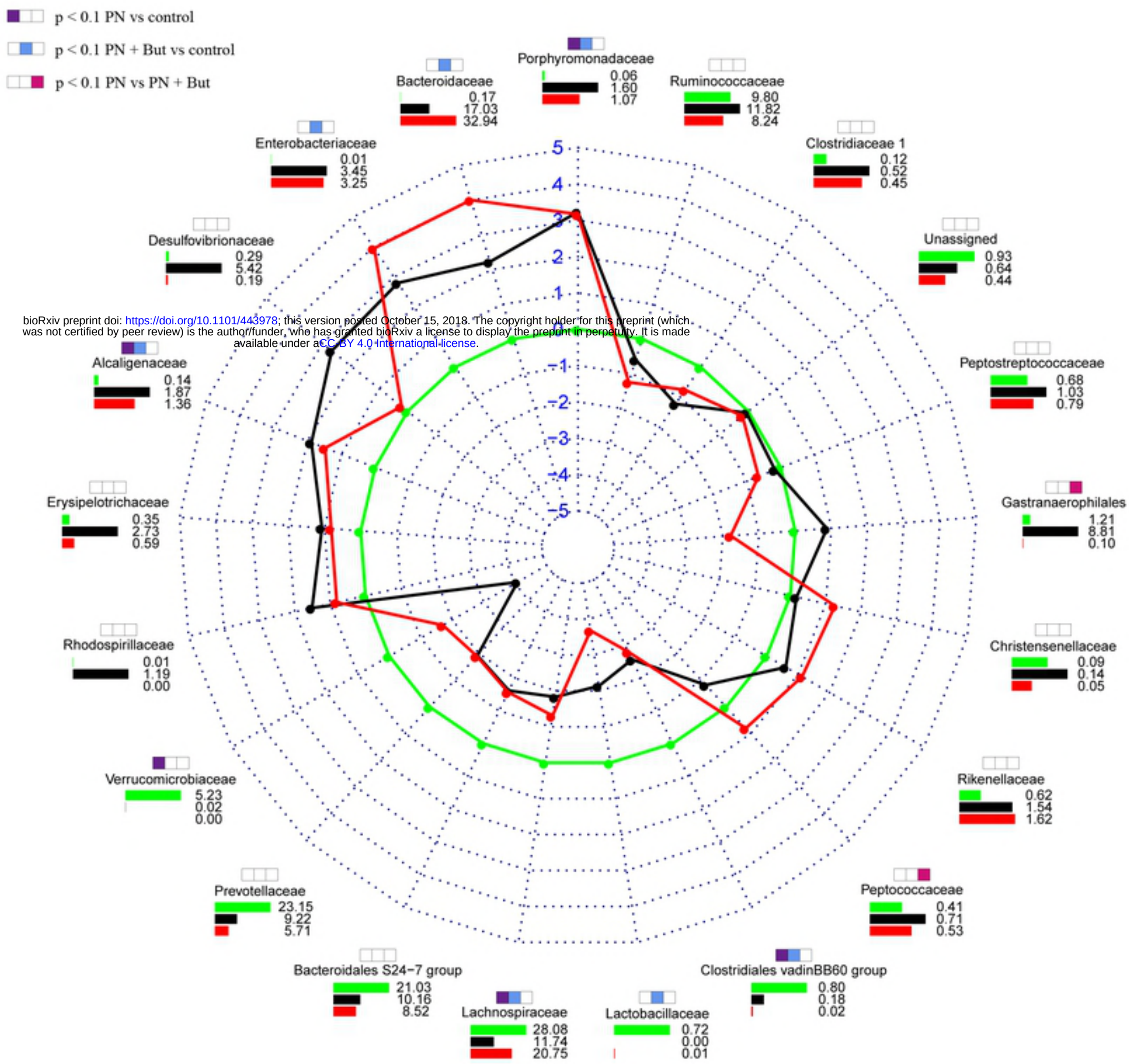

bioRxiv preprint doi: https://doi.org/10.1101/443978; this version posted October 15, 2018. The copyright holder for this preprint (which was not certified by peer review) is the author/funder, who has granted bioRxiv a license to display the preprint in perpetuity. It is made available under aCC-BY 4.0 International license.

Figure 8

bioRxiv preprint doi: https://doi.org/10.1101/443978; this version posted October 15, 2018. The copyright holder for this preprint (which was not certified by peer review) is the author/funder, who has granted bioRxiv a license to display the preprint in perpetuity. It is made available under aCC-BY 4.0 International license.

A

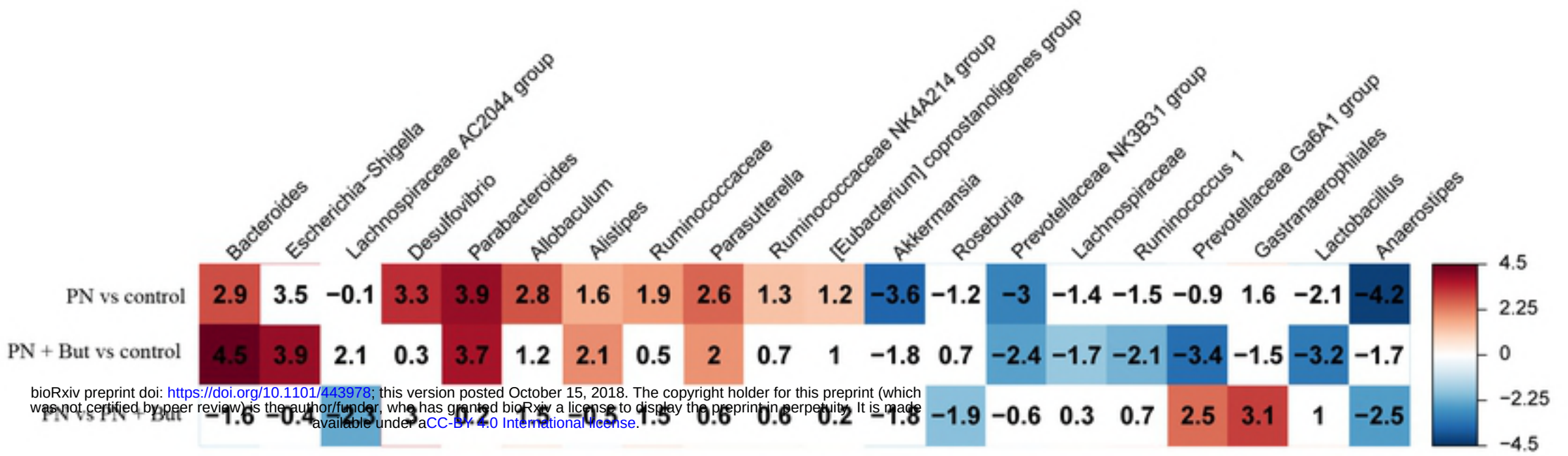

B

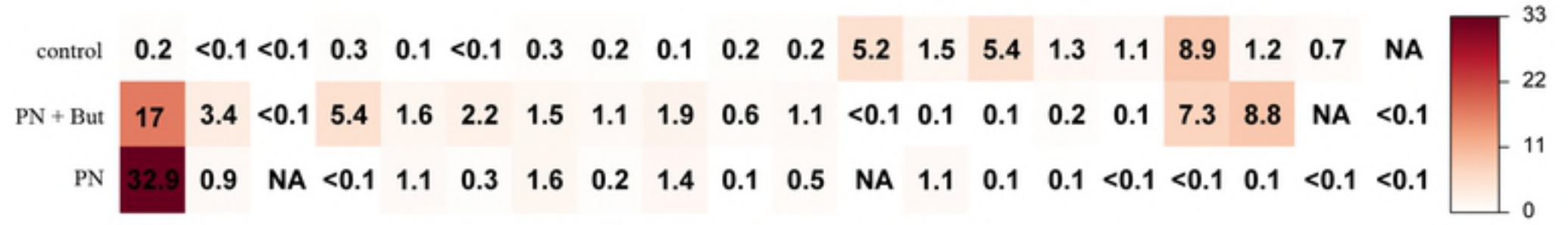

Figure 9